

# Preparation and Characterization of Magnetic Glass Ceramics Derived from Iron Oxides Bearing Rolling Mill Scales Wastes

Salwa AM Abdel-Hameed<sup>1</sup>, Ibrahim Hamed M<sup>2</sup>, Barbara J Muller-Borer<sup>3</sup> and Nehal A Erfan<sup>2</sup>

- 1 Glass Research Department, National Research Centre, 33 El Bohouthst. (former El Tahrirst.)-Dokki-Giza- P.O.12622 , Egypt
- 2 Chemical engineering department, faculty of engineering, Minia university, Minia, Egypt
- 3 Department of Engineering, East Carolina University, Greenville, NC, USA

## Abstract

Rolling Mill Scales (RSW) were used as raw materials for preparation of hard and soft magnetic glass ceramics which have a wide range of applications. In steel processing up to 5% of steel is lost with scales during the hot rolling operation where Iron oxides form ~ 69-72% of the milling scales weight. In addition to the iron content, mill scales are contaminated with remains of lubricants, oils and grease from the equipment associated with rolling operations. The oil content typically ranges from 0.1 and 2% -but can reach up to 20%-beside ~10% water. The goal of this project was to evaluate magnetic properties of soft and hard magnetic glass ceramics synthesized from RSW. To synthesize soft magnetic glass ceramics (SMGC) and hard magnetic glass ceramics (HMGC), 65 wt% and 37 wt% respectively of RSW were used. Quenching-melting technique was utilized. Differential thermal analysis (DTA) showed one broad exothermic peak at 906°C and at 731°C for SMGC and HMGC respectively. For SMGC, the major detectable peaks belong to Zn-ferrite ( $ZnFe_2O_4$ ) and Hematite ( $Fe_2O_3$ ) as shown by X-ray diffraction (XRD) analysis. Alternatively, Ba-hexaferrite ( $BaFe_{12}O_{19}$ ) and Hematite are the detected phases in HMGC samples. After heat treatment, crystallization of ~131-166 and 24-34 nm magnetic particles were detected for SMGC and HMGC via transmission electron microscopy (TEM). An increase in saturation magnetization from 18 emu/g for RSW to 66.5 emu/g for heat treated SMGC and 19 emu/g for HMGC was measured with a Vibrating Scanning Magnetometer (VSM). The results confirm that we were able to recycle rolling mill scales into hard and soft magnetic glass ceramics with magnetic phase content reaches 92.4 wt%.

**Keywords:** Rolling mill scales; Glass-ceramics; Nanoparticles; Ferrimagnetism; Zn-ferrite and Ba-hexaferrite

**Corresponding author:** Nehal A Erfan

✉ erfann14@ecu.edu

Chemical engineering department, faculty of engineering, Minia university, Minia, Egypt.

**Tel:** +1-252-412-1154

**Citation:** Abdel-Hameed SAM, Hamed IM, Muller-Borer BJ, et al. Preparation and Characterization of Magnetic Glass Ceramics Derived from Iron Oxides Bearing Rolling Mill Scales Wastes. *Nano Res Appl.* 2015, 1:1.

**Received:** September 02, 2015; **Accepted:** October 27, 2015; **Published:** November 05, 2015

## Introduction

The properties of nanomaterials are not well understood although they have been in use for centuries. Early Chinese dynasty porcelain glazes were the earliest application [1]. During the Renaissance period, artists in Umbria, Italy utilized nanomaterials in art fabrication [2]. Several decades ago, serious research on nanotechnology began [1]. Since then, significant improvements have been made on process development of nanomaterials with controlled structure and properties [1]. Recently, one-dimensional (1D) and quasi-one-dimensional (Q 1D) materials with magnetic phases have attracted great attention due to their potentials as building blocks for future electromagnetic devices [3,4].

The need for waste recycling is important as scientists continue to seek ways to reduce the environmental impact of industrial wastes. Industrial waste has been a major source of air, water and industrial pollution resulting from solid waste disposal. This consequently has a negative impact on the environment with increased associated costs. Owing to the growing amount of solid wastes produced by industrial firms, increased environmental regulations and the need for pollution abatement, there is increased interest in using recycling as a means of diverting solid wastes to useful products as glass-ceramics.

The following are examples for producing glass ceramics from solid wastes. Blast-furnace slag was the first silicate waste to be

investigated as a source material for glass ceramics. These slags consist of  $\text{CaO}$ ,  $\text{SiO}_2$  and  $\text{MgO}$  as the main constituents, with minor constituents such as  $\text{MnO}$ ,  $\text{Fe}_2\text{O}_3$  and  $\text{S}$ . The first attempt to commercialize a glass ceramic from slag was by the British Iron and Steel Research Association in the late 1960's [5]. Fabrication of glass-ceramics using slag-type wastes from non-ferrous metal production has been reported, these include copper slag [6,7] and phosphorus slag [8]. Up to 40 wt% of copper slag was incorporated into a base glass composition to produce tiles via the powder sintering method [6]. Mixtures of coal ash and waste glass have been used in early technological approaches to fabricate glass ceramics and glass matrix composites using powder technology and sintering [9-11]. Cheng *et al.* conducted single-step heat treatment of glasses obtained from vitrified incinerator fly ash [12] and of a mixture of electric arc furnace (EAF) dust and fly ash [13].

M Pelino *et al.* [14] and Morsi *et al.* [15] prepared glass specimens by melting mixtures of magnesite, feldspar, quartz sand, kaolin and cement dust with dust content in the range 25–37 wt%. Gorokhovskiy *et al.* [16] produced diopside-based glass ceramics based on a combination of a wide range of wastes (quartz-feldspar waste, limestone dust, phosphorus slurry, metallurgical slag) and selected commercially available chemicals, such as  $\text{Cr}_2\text{O}_3$ , as a nucleating agent. Yun *et al.* [17] prepared glass-ceramics from a mixture of fluorescent glass and waste shell in a weight ratio of 4:1. Diaz *et al.* [18] recently reported that it is possible to produce cordierite glass-ceramics from inorganic wastes of anodizing plants. Reusing jarosite and goethite from hydrometallurgical processes to obtain glass and glass-ceramic materials has been reported in several papers [19-25].

To our knowledge, production of magnetic glass ceramics from rolling mill scales has not been previously reported.

Rolling mill scales are solid by-products from the steel making industry that contain metallic iron and three types of iron oxides: Wustite, Hematite and magnetite. Rolling mill scales also contain traces of non-ferrous metals, alkaline compounds and oils from the rolling process [26]. Mill scales are formed on the outer surfaces of plates, sheets or other configurations produced by rolling red-hot iron or steel billets in rolling mills. Mill scales with bluish black color are composed of iron oxides mostly ferric (**Figure 1**). In the whole world, 13.5 million tons of mill scales are generated annually [27]. Depending on the process and the nature of the product, the weight of mill scale can vary between 20 and 50 kg/t of the hot rolled product. The average specific production of this by-product is typically 35-40 kg/t [28]. Approximately 90% of mill scales is directly recycled within the steel making industry and small amounts are used for ferroalloys, in cement plants and in the petrochemicals industry [29-32]. Volodymer *et al.* [26] utilized the rolling mill scales in the iron ore sintering process as they were able to improve the combustion of the scale's oil at the sintering process by preparation of a mixture with peat. By their method the consumption of the oiled scale was increased from zero to 12.8 kg. A study was made by MI Martin *et al.* [28] of the reduction of mill scale to sponge iron using coke at different temperatures. N.M. Gaballah *et al.*, [33] prepared two models for the production of iron from rolling mill scales wastes via hydrogen reduction at varying temperatures.



**Figure 1** Photograph of Rolling mill scales. (Composed of 69-72% iron oxides, 20%oil and 10%water).

Reintroducing the rolling mill scales into an industrial process through well planned programs will reduce their environmental impact and will improve cost savings.

Glass-ceramics are defined as composite materials that contain at least one crystalline phase dispersed in an amorphous glassy matrix. The chemical composition of the glass precursor influences the physical and chemical properties of the composite. Therefore, the investigation of new composite glass materials with controlled particles size distribution and aspect ratio has an impact on industry. Preparation of magnetite-containing glass ceramics has been reported by several groups [34-36] where ferromagnetic bio glass-ceramics containing 45 wt% of magnetite were prepared [37] and about 60 wt% were reported by others [38,39]. Traditional compact magnetic materials are commonly prepared by sintering of ferrite powders [40,41] with a mean particle size of about 1  $\mu\text{m}$  at 1200-1250°C. During sintering the magnetic crystals grow so that multi-domain behavior occurs which lowers the coercivity of the material [42].

Spinel and hexa-ferrites are a large important class of materials with the general formula  $\text{M-Fe}_2\text{O}_4$  for spinel ferrites and  $\text{M-Fe}_{12}\text{O}_{19}$  for hexa-ferrites, where M is a divalent cation. Hexa-ferrites have a hexagonal crystal structure where the magnetic properties of the spinel ferrites originate mainly from the magnetic interactions between cations with magnetic moments, which are situated in tetrahedral and octahedral sites [43-45]. The prepared materials have wide spread applications in material science [40,46-51] and biotechnology [38,39,52].

In this study, glass techniques were used to prepare a compact body in which magnetic particles were well dispersed and kept in single domain behavior. We prepared compact glass ceramics that contain single domain particles (<100 nm) separated by a nonmagnetic matrix which lowers the sinter temperature, prevents the particles from growing to be in multi-domain and resulted in low magnetic interaction. The main objective of this research was to evaluate RSW from various metallurgical

industries and to prepare soft and hard nanomagnetic glass-ceramics.

These nanomagnetic glass-ceramics have potential applications in health care such as cell separation, magnetic resonance imaging contrast agents [53], drug delivery, tissue engineering and hyperthermia treatment of cancer. In addition, they have a wide range of applications in information storage systems [54], ferrofluid technology [55,56], magnetocaloric refrigeration, gas-sensors and catalysis [57].

## Experimental Methods

### Preparation of the glass

X-Ray Fluorescence (XRF) analysis was used to determine the composition of the RSW samples as illustrated in **Table 1**. The samples were prepared with two compositions: one based on crystallization of  $ZnFe_2O_4$  as a soft magnet and the other based on  $BaFe_{12}O_{19}$  as a hard magnet. The compositions of the prepared samples are reported in **Table 2**. RS and RH are soft and hard magnetic reference samples prepared from pure chemicals such as  $ZnCO_3$ ,  $Na_2CO_3$ ,  $NH_4H_2PO_4$ ,  $TiO_2$ ,  $BaCO_3$ ,  $H_3BO_3$  and  $SiO_2$ . SMGC refers to soft magnetic glass ceramics that contain about 65% of RSW while HMGC refers to hard magnetic glass ceramics that contain 37% of RSW. Small amounts of ZnO as  $ZnCO_3$ ,  $Na_2O$  as  $Na_2CO_3$ ,  $P_2O_5$  as  $NH_4H_2PO_4$ ,  $TiO_2$ , BaO as  $BaCO_3$  and  $B_2O_3$  as  $H_3BO_3$  were added to complete the design of the desired phases. As previously described (Salwa A. M. Abdel-Hameed et al. 2014) the samples were prepared by melting the required amounts of reagent grade chemicals with composition shown in **Table 2**. Samples were prepared in platinum crucibles at 1500°C for soft ferrite samples and 1200°C for hard ferrites, and heated for 2 h in electrically heated furnace with occasional swirling every 30 min to ensure homogenization. The melts were poured onto a stainless steel plate in 1-2 mm thick strips by applying another cold steel roller.

### Characterization

**Table 1** Quantitative analysis(XRF) of rolling mill scales waste raw material(RSW).

Main Constituents	(wt,%)
$SiO_2$	1.33
$TiO_2$	0.03
$Al_2O_3$	0.45
$Fe_2O_3^{tot.}$	95.56
MgO	0.15
MnO	0.82
CaO	1.22
$Na_2O$	0.11
$K_2O$	0.05
$P_2O_5$	0.06
Cl	0.048
CuO	0.034
NiO	0.012
$Cr_2O_3$	0.049
$V_2O_5$	0.038
ZnO	0.049

To determine the temperatures of the glass transition ( $T_g$ ) and crystallization ( $T_c$ ) of the glass samples differential thermal analysis (DTA; SDTQ600) under inert gas with a heating rate of 10°C/min was used. Alumina was used as the inert reference material. The results obtained served as a guide for determining the required heat-treatment temperatures needed to induce crystallization in the samples. To investigate the effect of heat treatment on the phase transformation and sample properties, samples were heat treated at 900°C for 2 h. Samples before and after heat treatment were evaluated using powder X-ray diffraction using a Ni-filled  $Cu-K\alpha$  target to identify their content and the precipitated crystalline phases. X-ray diffraction (XRD) was performed using Bruker D8 Advanced instrument (Germany D8 ADVANCE Cu target 1.54 Å, 40 KV, 40 mA). The reference data for the interpretation of the XRD patterns was obtained from ASTM X-ray diffraction card files. Samples were crushed and sonically suspended in ethanol. A few drops of the suspended solution was placed on an amorphous carbon film held by a copper micro grid mesh. The microstructure and crystallite size was characterized using a TEM 2010 transmission electron microscope. Chemical composition of the crystals in the glass ceramics were analyzed by EDX using Oxford instrument INCA-sight on a Joel TXA-840A electron probe micro analyzer. The magnetic properties were evaluated with a vibrating sample magnetometer (VSM, 9600-1 LDJ, USA) in a maximum applied field of 20 KOe. Saturation magnetization ( $M_s$ ), remanance magnetization ( $M_r$ ) and coercivity ( $H_c$ ) were determined from the hysteresis loops.

## Results and Discussions

### Differential thermal analysis

The DTA scan provides a rapid method to investigate the crystallization nature, the effect of heat and the temperature range of crystallization and the proper heat-treatment schedule. The limits of crystallization however, are about  $\pm 30^\circ C$  of the DTA crystallization peaks; as with powdered glass samples, surface nucleation and devitrification tend to obscure the internal structural changes of the glass [58].

DTA of RS, SMGC, RH and HMGC samples before heat treatment are shown in **Figure 2**. The materials resemble a crystalline state. When the amorphous state decreases, the endothermic and exothermic intensities decrease. In general, DTA results show lower intensity thermal effects due to the high degree of crystallization during cooling from melting temperature to room temperature. DTA results show an endothermic effect resembling an amorphous phase at 657°C for RS, 642°C for SMGC sample, 551°C for RH and about 516°C for HMGC sample. This endothermic reaction is believed to be caused by an increase in heat capacity due to transformation of glass from a rigid to plastic structure and the accompanied rearranging of different atoms as a precrystallization step [59]. The endothermic temperatures are lower in the batch compositions containing RSW than those of pure chemicals due to the reflux effect of different oxides present in RSW which lower the samples viscosity and  $T_g$  as shown in **Table 2**. The sharp endothermic effect at 90°C in SMGC was attributed to water evaporation while the broad exothermic peak at 906°C is an indication for crystallization of both hematite and Zn-ferrite

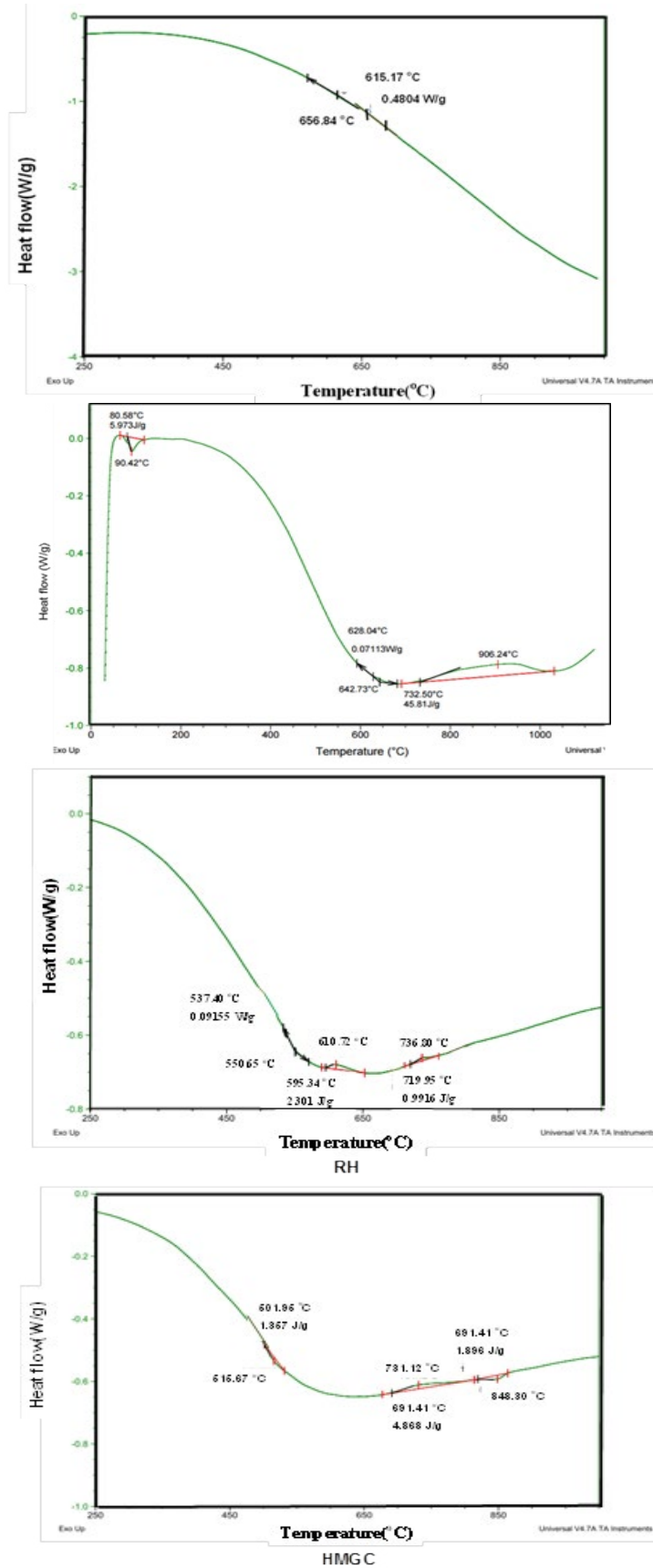


**Figure 2** DTA of RS, SMGC, RH and HMGC samples (Illustrating endothermic and exothermic peaks which are evidence of crystallization process).

**Table 2** Chemical composition in wt% of prepared magnetic glass ceramics.

Chemical Composition wt%	Sample ID			
	RS	SMGC	RH	HMGC
Fe <sub>2</sub> O <sub>3</sub>	70.5	68.38	43.17	40.21
SiO <sub>2</sub>	-	0.952	4.64	4.713
TiO <sub>2</sub>	2.21	2.168	-	0.0126
ZnO	23.96	23.14	-	-
Al <sub>2</sub> O <sub>3</sub>	-	0.322	-	0.1863
MgO	-	0.107	-	0.0631
CaO	-	0.873	-	0.51
Na <sub>2</sub> O	2.21	2.23	-	0.463
K <sub>2</sub> O	-	0.036	-	0.21
P <sub>2</sub> O <sub>5</sub>	1.1	1.12	-	0.025
CuO	-	0.024	-	0.0143
Cr <sub>2</sub> O <sub>3</sub>	-	0.035	-	0.02
MnO	-	0.587	-	0.345
B <sub>2</sub> O <sub>3</sub>	-	-	10.76	14.632
BaO	-	-	41.43	38.59
Ni <sub>2</sub> O	-	<b>0.00859</b>	-	0.00505
V <sub>2</sub> O <sub>5</sub>	-	0.027	-	-

as confirmed by X- ray later. The absence of exothermic effect in RS sample indicates a high degree of crystallization during cooling from melting temperature to room temperature.

Alternatively, a single exotherm appeared at 731°C for the HMGC sample and two exothermic peaks at 611°C and 737°C in RH sample corresponding to Ba-hexaferrite crystallization. The shape and intensity of the exothermic peak are a good indicator for the crystallization process; the sharper and stronger exothermic peak reflects larger and quicker crystallization, conversely, if the exothermic peak is broad, the crystallization is slow and small [60]. The DTA results were used to determine heat treatment schedule which was applied to samples at 900°C for 2 h to study its effect on the crystallization process.

### X-ray diffraction analysis

**Figure 3** depicts the correlation between the XRD results of RSW , Rs and SMGC before and after heat treatment, While **Figure 4** depicts the correlation between RSW,RH and HMGC before and after heat treatment.

The major detectable peaks can be indexed to Zn-ferrite (ZnFe<sub>2</sub>O<sub>4</sub>) and Ba-hexaferrite (BaFe<sub>12</sub>O<sub>19</sub>) for SMGC and HMGC samples respectively. These designed composition succeeded in reaching the targeted phases. Several factors contribute to the broadening of peaks in X-ray diffraction [60,61]. For example, factors related to the resolution and the incident X-ray wavelength of the XRD, as well as the sample crystallite size and non-uniform microstrain, can cause a line broadening. In the case of an instrumental broadening, the line width will vary smoothly with 2θ or d spacing. On the other hand, the line broadening originating from the sample characteristics will have a different relationship. Using Scherrer's equation [62,63] for crystallite size and the Bragg's law for diffraction [64], crystallite size and microstrain components are estimated :

• The Scherer equation is: 
$$\tau = \frac{K\lambda}{\beta \cos \theta}$$

where:

- $\tau$  is the mean size of the ordered (crystalline) domains, which may be smaller or equal to the grain size;
- $K$  is a dimensionless shape factor, with a value close to unity. The shape factor has a typical value of about 0.9, but varies with the actual shape of the crystallite;

$\lambda$  is the X-ray wavelength;

$\beta$  is the line broadening at half the maximum intensity (FWHM), after subtracting the instrumental line broadening, in radians. This quantity is also sometimes denoted as  $\Delta(2\theta)$ ;

$\theta$  is the Bragg angle.

• Bragg's law is:  $2d \sin \theta = n\lambda$

where

- $n$  is a positive integer

$\lambda$  is the wavelength of incident wave

$d$  is the spacing

**Figure 3a** illustrates the difference between RSW and SMGC before and after heat treatment. The RSW samples include Hematite and Magnetite phases with trace Wuestite phase which disappeared completely in SMGC. Furthermore, applying heat treatment at 900°C for 2 h affected the crystallization of Zn-ferrite as a unique phase. Comparing the main peaks in the three patterns we notice that heat treatment has a greater effect on crystallization and amount of Zn-ferrite crystallized. The XRD spectra represent the crystallization of Zn-ferrite as a single phase in RS sample (**Figure 3b**), with less crystallization relative to SMGC sample. The amount of Zn-ferrite decreased in the RS sample after heat treatment at 900°C for 2 h due to the separation of SiO<sub>2</sub> phase. Comparing the compositions of RS and SMGC, it's evident that there are extra oxides present in SMGC sample due to RSW composition as listed in **Table 2**. These oxides facilitate the crystallization of Zn-ferrite

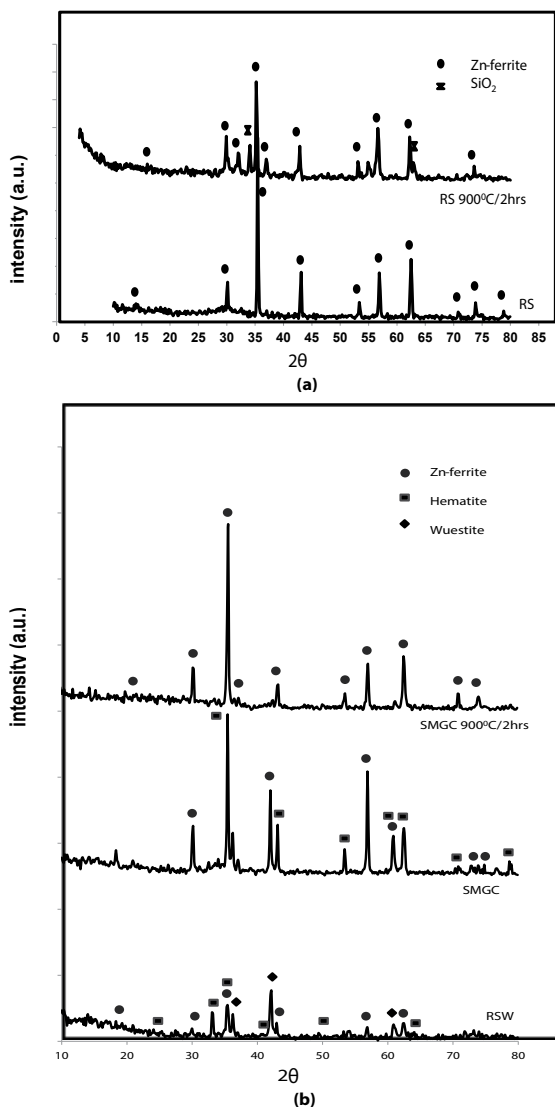


**Figure 3** XRD spectra of glass-ceramics before and after heat treatment, a) RS samples before and after heat treatment and b) SMGC before and after heat treatment.

by decreasing the viscosity of the sample and increasing mobility of ions to crystallize in the quenched sample.

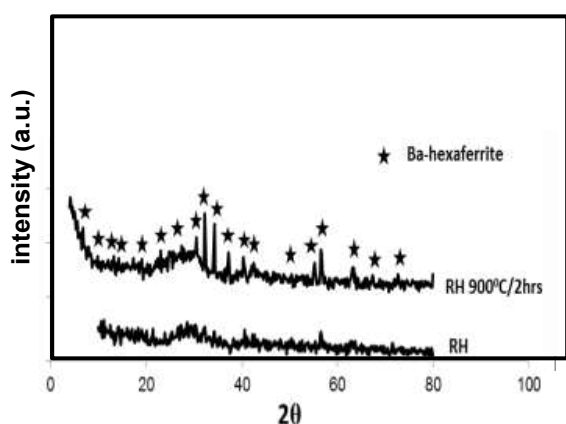
Alternatively, **Figure 4b** shows the XRD spectra of HMGC before and after heat treatment. Hematite, Wuestite and Zn-ferrite phases present in the RSW sample disappear and a broad hump characterizing the amorphous glassy state appears in HMGC sample before heat treatment. Ba-hexaferrite crystallizes as the sole formed magnetic phase in a nonmagnetic matrix when the sample is exposed to heat treatment at 900°C for 2 h. A clear effect of the heat treatment on the RH sample is shown in **Figure 4a**, with the transformation from an amorphous to crystalline state as represented by crystallization of pure Ba-hexaferrite. More Ba-hexaferrite crystallized in HMGC than in the RH which is reflected by higher XRD peak intensities.

## Transmission electron microscope

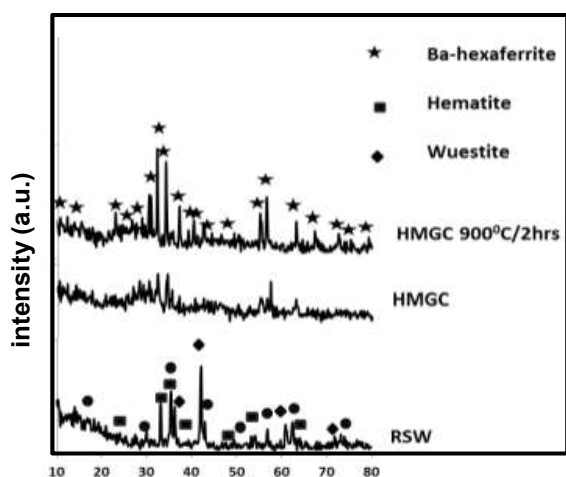
To investigate the possibility of micro twinning and the homogeneity of the materials TEM was performed. Particle size was measured from TEM images. **Figure 5** shows the TEM microstructures in high magnification for SMGC, RS, HMGC and RH samples before and after heat treatment. **Figure 5a,5b** show the precipitation of nanosized cubic crystals of Zn-ferrite and Hematite phases in the SMGC sample before heat treatment with crystalline size range from 131-166 nm. All Hematite crystals transformed to Zn-ferrite after heat treatment with crystalline size range from 23-33 nm, this confirmed the results obtained from XRD calculations shown in **Figure 3**. TEM for RS samples are shown in **Figure 5c, 5d** which illustrates the transformation of Zn-ferrites to SiO<sub>2</sub> phase with crystalline size of about 223 nm after heat treatment. In contrast, Ba-hexaferrite with hexagonal crystals is formed as a unique phase with crystalline size ranging from 24-34 nm in HMGC samples after heat treatment as shown in **Figure 4**. In addition, TEM for RH represented in **Figure 5g, 5h** show the crystallization of Ba-hexaferrite as a single phase with crystalline size ranging from 2-12 nm after heat treatment.

## Magnetic properties

**Figures 6 and 7** illustrate the room temperature magnetic hysteresis (M-H) loops of SMGC, RS, HMGC and RH samples before and after heat treatment under a magnetic field strength of  $\pm 20$  KOe. **Table 3** lists the relevant magnetic parameters; saturation magnetization ( $M_s$ ), coercivity ( $H_c$ ), remanence ( $M_r$ ) obtained from M-H loops. The magnetic field necessary to saturate the samples increased with the increase in the crystallization of Zn-ferrite in soft samples and Ba-hexaferrite in hard magnets. **Figure 6** illustrates that  $M_s$  increased from 18.393 emu/g for RSW, to 45.175 emu/g for SMGC samples before heat treatment and continued increasing to 66.463 emu/g after heat treatment. In contrast, the magnetization of RS samples declined from 38.678 emu/g to 24.293 emu/g after being exposed to heat treatment at 900°C for 2h. **Figure 7** shows that  $M_s$  increased from 18.393 emu/g for RSW sample to 19.06 emu/g for HMGC sample and increased to 24.19 emu/g after heat treatment. The same trend is shown for RH samples where  $M_s$  increased from 8.0774 emu/g to 16.665 emu/g after heat treatment for 900°C/2 hrs. As expected, saturation magnetization in the samples is shown to be directly proportional to the degree and amount of crystallization of Zn-ferrite and Ba-hexaferrite. It should be noted that Zn-ferrites and Ba-hexaferrite are ferromagnetic materials, whereas hematite is an antiferromagnetic. The results show that hematite and amorphous phases have a very low saturation magnetization. As a consequence, the variation of the saturation magnetization can be attributed to the modification of the quantity of Zn-ferrite and Ba-hexaferrite crystals [65] present in the glass-ceramic samples. Therefore, the maximum magnetization values of 66.463 emu/g for SMGC after heat treatment and 24.19 emu/g for HMGC after heat treatment refer to the heaviest and most intense Zn-ferrite and Ba-hexaferrite crystallization of all the soft and hard magnet samples respectively. The quantity of the magnetic phase present in the glass ceramic samples was determined from the saturation magnetization ratio between the sample and pure magnetite ( $M_s=72$  emu/g) [66]. 92 emu/g is the saturation magnetization of



(a)



(b)

**Figure 4** XRD spectra of glass-ceramics before and after heat treatment, a) RH samples before and after heat treatment and b) HMGC before and after heat treatment.

bulk magnetite as reported from the literature [67], O. Bretcanuet. el. Measured the magnetite saturation magnetization as 72 emu/g and they referred this decrease to the powder form of the measured samples. Surface effects can modify the saturation magnetization of a magnetic material, usually lowering the magnetization. The maximum magnetic phases accumulation is 92.4 wt% for heat treated SMGC which is a big increase than what previously reported by other workers [37-39].

The coercivity of soft ferrimagnetic glass ceramics varied between 106.25 Oe for the RSW sample and 32.775 Oe for SMGC before heat treatment with a small increase to 32.966 Oe after heat treatment. In HMGC samples heat treatment had a larger effect on coercivity which increased from 106.25 G for RSW sample to 128.77 G for the melted HMGC samples before heat treatment

and increased to 425.32 G after heat treatment. Similarly, heat treatment had a noticeable effect on the reference samples coercivities with an increase from 16.756 G to 193.44 G after heat treatment of RS and increased from 160.39 G to 1001.5 G for RH after heat treatment. The coercivity of a ferrimagnetic material is the intensity of the applied magnetic field required to reduce the magnetization of that material to zero after the magnetization of the sample has been driven to saturation. Coercivity measures the resistance of a ferromagnetic material to become demagnetized. The wide range of coercivity provides for a wide range of applications. Materials with high coercivity, which are called hard ferromagnetic materials, are used to make permanent magnets. Permanent magnets are used in electric motors, magnetic recording media (e.g., hard drives, floppy disks, or magnetic tapes) and magnetic separation. While materials with low coercivity which are said to be soft magnets may be used in microwave devices, magnetic shielding, transformers, or recording heads. The retentivity is found to detect the amount of magnetic materials which can be magnetized [68,69], even in the absence of external magnetic field. In comparison between soft and hard ferrites, **Table 3** shows that the retentivity of most of the hard magnets is larger than that of the soft magnets and is related to the area of the hysteresis loops. The area of the hysteresis loops of the hard ferrites is larger than the areas in the case of soft ferrites. The area under the hysteresis loop is proportional to the energy loss and hence the heat generated by a sample under an alternating field and hard ferrites samples are capable of generating more heat. The large variation in the area under the loops for hard and soft ferrites samples provides a controlled heat generation by appropriate choice of sample.

## Conclusions

- Two different ferrimagnetic glass ceramics with compositions based on crystallization of Zn-ferrite as soft magnet and Ba-hexaferrite as hard magnet were prepared.
- The influence of the chemical composition, the amount of Zn-ferrite and Ba-hexaferrite crystallization and the microstructure of ferromagnetic glass ceramics on magnetic properties of glass ceramics were investigated.
- The Heat treatment schedule of 900°C for 2 h enhanced the crystallization of Zn-ferrite in soft glass ceramics and Ba-hexaferrite in hard magnetic glass ceramics.
- Nanomagnetic hexaferrite was obtained in the range 24-34 nm.
- From the magnetic measurements, we conclude that heat treated SMGC had the highest magnetization of 66.5 emu/g and has 92.4 wt% of magnetic phases.

## Acknowledgment

This work was supported financially by the Science and Technology Development Fund (STDF), Egypt, Grant no. 1044.

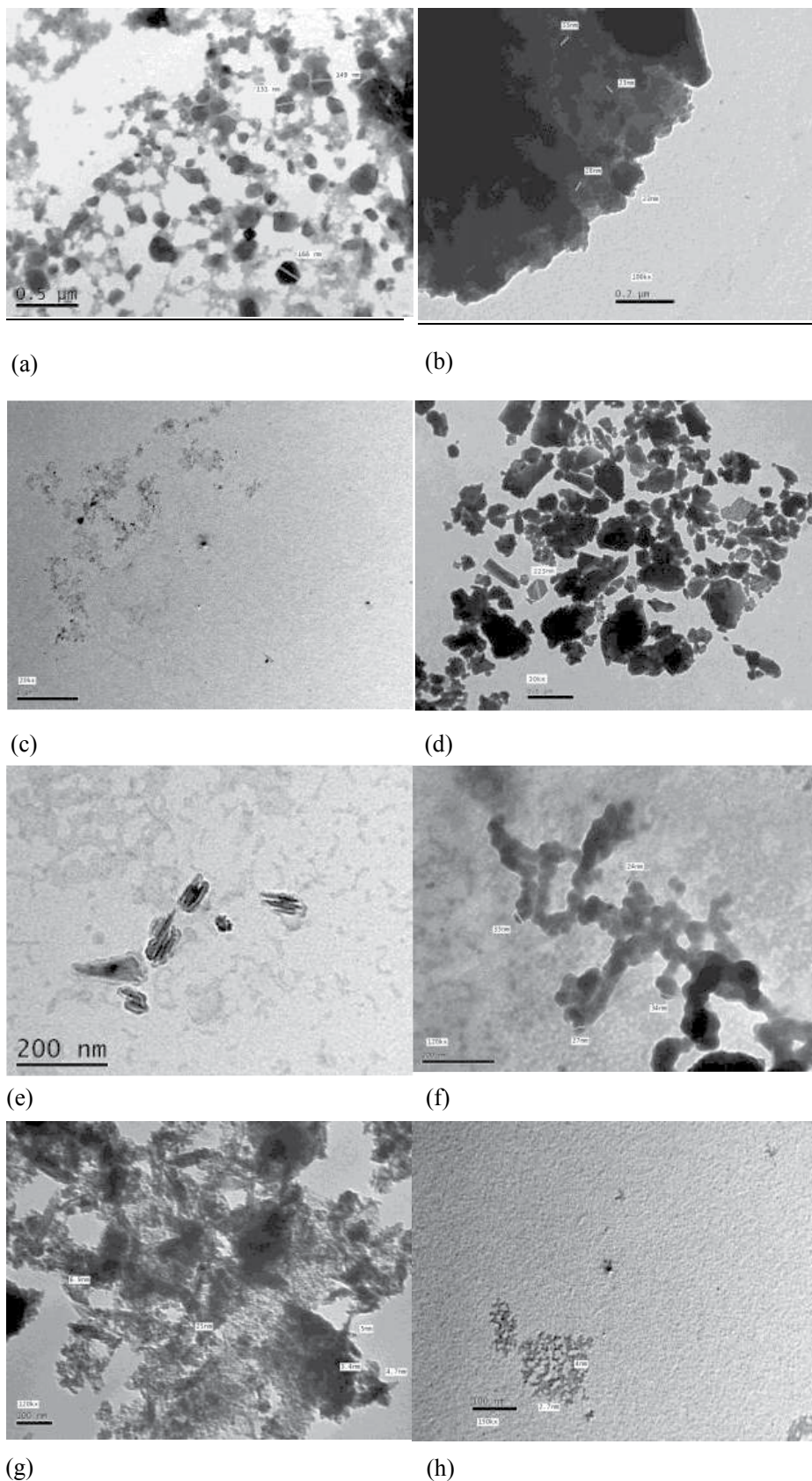


**Figure 5** TEM images of samples before and after heat treatment.

a) quenched SMGC, b) heat treated SMGC, c) quenched RS, d) heat treated RS, e) quenched HMGC, f) heat treated HMGC, g) quenched RH and h) heat treated RH samples.

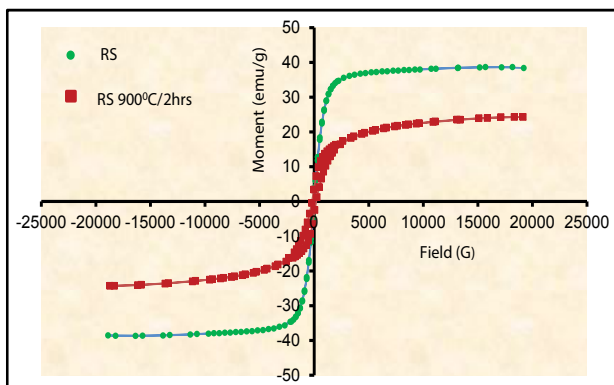
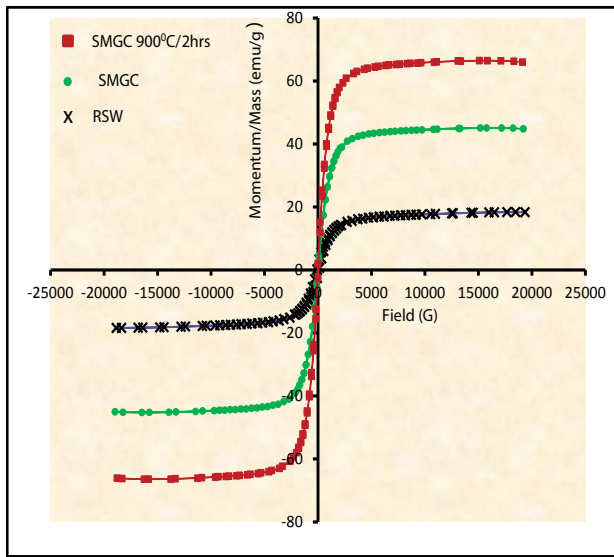


**Figure 6** Magnetization curves of RSW, SMGC and RS samples before and after heat treatment.

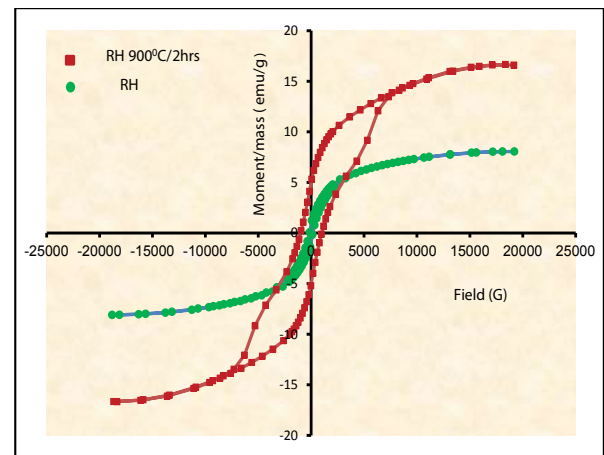
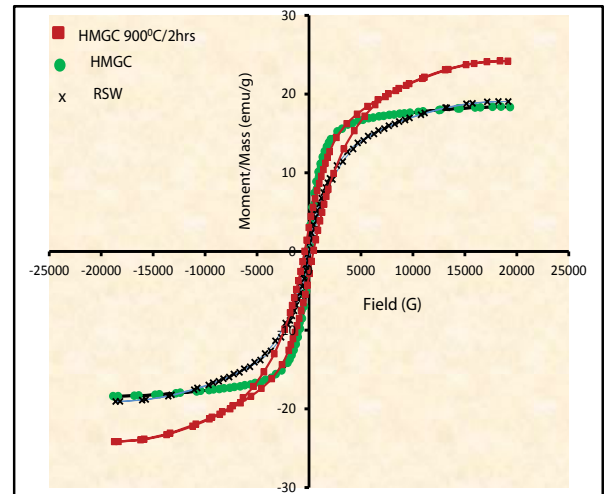


**Figure 7** Magnetization curves for RSW, HMGC and RH samples before and after heat treatment.

**Table 3** Magnetic properties of RSW, RS, RH, SMGC and HMGC glass ceramics before and after heat treatment.

Sample ID	Magnetization (emu/g)	Coercivity(G)	Retentivity(emu/g)
RSW	18.393	106.25	1.6785
RS	38.678	16.756	0.73946
SMGC	45.175	32.775	1.4215
RS 900°C/2hrs	24.293	193.44	3.7014
SMGC 900°C/2hrs	66.463	32.966	2.3594
RH	8.0774	160.39	0.92542
HMGC	19.06	128.77	0.95886
RH 900°C/2hrs	16.665	1001.5	5.0392
HMGC 900°C/2hrs	24.19	425.32	3.1612

## References

- 1 Ramaseshan R, Sundarrajan S, Jose R (2007) Nanostructured ceramics by electrospinning. *Journal of applied physics* 102: 111101.
- 2 Padeletti G, Fermo P (2003) Italian Renaissance and Hispano-Moresque lustre-decorated majolicas: imitation cases of Hispano-Moresque style in central Italy. *Applied physics A: material science process* 77: 125-133.
- 3 Seshadri R (2005) Zinc oxide-based diluted magnetic semiconductors. *Current Opinion in Solid State and Material science* 9: 1-7.
- 4 Yang JH, Zhao LY, Zhang YJ, Wang YX, Liu HL (2008) Paramagnetic behavior of  $Zn_{1-x}Mn_xO$  at room temperature. *Cryst Res Technol* 43: 999-1003
- 5 Davies MW, Kerrison B, Gross WE, Robson WJ, Wichell DF (1970) *J Iron Steel Institute* 208-348.
- 6 Marghussian VK, Maghsoodipoor A (1999) Fabrication of unglazed floor tiles containing Iranian copper slags. *Ceramics International* 25: 617-622.
- 7 Omar AA, L-Gamal MAE, Kotb W, Mahmoud MM (2000) The Use of Copper Slags for Making Glass-Ceramics. *Glass Science and Technology Suppl* 73: 51-58.
- 8 Murat M, Martel S, Bouster C (1990) optimization of devitrification processing in the field of glass ceramics example of the devitrification of phosphorous slag. *Ceramics International* 16: 171-175.
- 9 Boccaccini AR, Bucker M, Bossert M (1996) Glass and glass-ceramics from coal fly-ash and waste glass. *Tile and Brick International* 12: 515-518
- 10 Boccaccini AR, Bucker M, Bossert J, Marszalek K (1997) Glass matrix composites from coal flyash and waste glass. *Waste Management* 17: 39-45.
- 11 Boccaccini AR, Janczak J, Kern H Ondracek G (1993) in *Proc. 4th. International Symposium on the Reclamation, Treatment and Utilization of Coal Mining Wastes, Vol. II.* edited by K. M. Skarzynska, 719
- 12 Cheng TW, Chen YS (2003) On formation of  $CaO-Al_2O_3-SiO_2$  glass-ceramics by vitrification of incinerator fly ash. *Chemosphere* 51: 817-824.
- 13 Cheng TW (2003) Combined glassification of EAF dust and incinerator fly ash. *Chemosphere* 50: 47-51.
- 14 Pelino M, Karamanov A, Pisciella P, Crisucci S, Zonetti D (2002) Vitrification of electric arc furnace dusts. *Waste Management* 22: 945-949.
- 15 Morsi MM, Khater GA, Range KJ (2001) Glass ceramics in the system diopside-anorthite-orthoclase prepared by using some industrial waste materials. *Glass Technology* 42: 160-164.
- 16 Gorokhovskiy, Escalante-Garcia JI, Gorokhovskiy V, Mescheryakov D (2002) Inorganic Wastes in the Manufacture of Glass and Glass-Ceramics: Quartz-Feldspar Waste of Ore Refining, Metallurgical Slag, Limestone Dust, and Phosphorus Slurry. *Journal of the American Ceramic Society* 85: 285-287.
- 17 Yun YH, Yoon CH, OH JS, Kim SB, Kang BA, et al. (2002) Waste fluorescent glass and shell derived glass-ceramics. *Journal of Materials Science* 37: 3211-3215
- 18 Diaz B, Salgado S, Jordan R, Cruz E, Zayas ME (2003) Glass-Ceramics Made from Anodizing Plant Industrial Waste. *American Ceramic Society Bulletin* 9601-9604.
- 19 Pelino M, Cantalini C, Rincon JMA (1997) Preparation and properties of glass-ceramic materials obtained by recycling goethite industrial waste. *Journal of Materials Science* 32: 4655-4660.
- 20 Romeo M, Rincon JMA (1999) Surface and Bulk Crystallization of Glass-Ceramic in the  $Na_2O-CaO-ZnO-PbO-Fe_2O_3-Al_2O_3-SiO_2$  System Derived from a Goethite Waste. *Journal of the American Ceramic Society* 82: 1313-1317.
- 21 Marabini AM, Plescia P, Maccari D, Burrigato F, Pelino M (1998) New materials from industrial and mining wastes: glass-ceramics and glass- and rock-wool fiber. *International Journal of Mineral Processing* 53: 121-134.
- 22 Romeo M, Rincon JMA (1998) Effect of Iron Oxide Content on the Crystallization of a Diopside Glass-Ceramic Glaze. *Journal of the European Ceramic Society* 22: 883-890.
- 23 Karamanov A, Taglieri G, Pelino M (1999) Iron-Rich Sintered Glass-Ceramics from Industrial Wastes. *J Am Ceram Soc* 82: 3012-3016.
- 24 Pelino M (2000) Recycling of zinc-hydrometallurgy wastes in glass and glass ceramic materials. *Waste Management* 20: 561-568.
- 25 Pisciella P, Crisucci S, Karamanov A, Pelino M (2001) Chemical durability of glasses obtained by vitrification of industrial wastes *Waste Management* 21: 1-9.
- 26 Volodymyr I Shatokha, Oleg O Gogenko, Stanislav M Kripak (2011) Utilising of the oiled rolling mills scale in iron ore sintering process. *Resources Conservation and recycling* 55: 435-440.
- 27 Cho S, Lee J (2008) Metal Recovery From Stainless Steel Mill Scale by Microwave Heating. *Metals and Materials International* 14: 193-196
- 28 Martín MI, López J, Jose M Torralba (2012) production of sponge iron powder by reduction of rolling mill scale. *iron making& steelmaking* 39: 155-162.
- 29 Cho Young-Ki (1991) Making method for ferrite used mill/scales, Patent KR 9103783.
- 30 Osing D (1996) Reuse of metallurgical fines, Patent WO 96/31630.
- 31 Fleischander A, Pesl J, Gerbert W (1999) Aspect of recycling of steelworks by-products through the BOF. *SEAI Quarterly* 28: 51-60.
- 32 Poulalion A (2001) Process of recycling mill scale of alloyed steel in an electric furnace into a ferro-silicon product, Patent EP 1122319.
- 33 Gaballah NM, Zikry AF, Khalifa MG, Farag AB, El-Hussiny NA (2013) *Journal of Inorganic Non-Metallic Materials* 3: 23-28
- 34 Ebisawa Y, Miyaji F, Kokubo T, Ohura K, Nakamura T (1997) Surface reaction of bioactive and ferrimagnetic glass-ceramics in the system  $FeO-Fe_2O_3-CaO-SiO_2$ . *J Ceram Soc Jpn* 105: 947-951.
- 35 O'Horo M, Steinitz R (1968) Characterization of devitrification of an iron-containing glass by electrical and magnetic properties. *Mater Res Bull* 3: 117-125.
- 36 Auric P, Dang NV, Bandyopadhyay AK, Zarzycki J (1982) Superparamagnetism and ferrimagnetism of the small particles of magnetite in a silicate matrix. *J Non-cryst Solids* 50: 97-106.
- 37 Bretcanu O, Spriano S, Verne E, Coisson M, Tiberto P, et al. (2005) The influence of crystallized  $Fe_3O_4$  on the magnetic properties of coprecipitation-derived ferromagnetic glass-ceramics. *Acta Biomater* 1: 421-429.
- 38 Abdel-Hameed SAM, Hessien MM, Azooz MA (2009) Preparation and characterization of some ferromagnetic glass-ceramics contains high quantity of magnetite. *Ceram Int* 35: 1539-1544.

- 39 Abdel-Hameed SAM, Abeer M Elkady (2012) Effect of different additions on the crystallization behavior and magnetic properties of magnetic glass-ceramic in the system  $\text{Fe}_2\text{O}_3\text{-ZnO-CaO-SiO}_2$ . *J Adv Mater* 3: 167-175.
- 40 Shirk BT, Buessem WR (1970) Magnetic properties of barium ferrite formed by crystallization of a glass. *J Am Ceram Soc* 53: 192-196.
- 41 Gornert P, Sinn E, Schuppel W, Pfeiffer H, Rosler M, et al. (1990) Structural and magnetic properties of  $\text{BaFe}_{12-2x}\text{Co}_x\text{Ti}_x\text{O}_{19}$  powders prepared by the glass crystallization method. *IEEE Trans Magn* 26: 12-14.
- 42 Cetas TC, Gross EJ, Contractor Y (1998) A ferrite core/metallic sheath thermoseed for interstitial thermal therapies. *IEEE Trans Biomed Eng* 45: 68-77.
- 43 Evans BJ, Hafner SS, Weber HP (1971) Electric field gradients at Fe in  $\text{ZnFe}_2\text{O}_4$  and  $\text{CdFe}_2\text{O}_4$ . *J Chem Phys* 55: 5282.
- 44 Att-Allah SS, Fayek MK (2000) Effect of Cu substitution on conductivity of Ni-Al ferrite. *J Phys Chem Solids* 61: 1529-1534
- 45 Mahmoud MH, Hamdeh HH, Ho JC, O'Shea MJ, Walker JC (2000) Mössbauer studies of manganese ferrite fine particles processed by ball-milling. *J Magn Magn Mater* 220: 139-146.
- 46 Muller R, Ulbrich C, Schuppel W, Steinmetz H, Steinbeib E (1999) Preparation and properties of barium-ferrite-containing glass ceramics. *J Eur Ceram Soc* 19: 1547-1550.
- 47 Lee CK, Speyer RF (1994) Glass formation and crystallization of barium ferrite in the  $\text{Na}_2\text{O-BaO-Fe}_2\text{O}_3\text{-SiO}_2$  system. *J Mater Sci* 29: 1348-1351.
- 48 Sohn SB, Choi SY, Shim IB (2002) Preparation of Ba-ferrite containing glass-ceramics in  $\text{BaO-Fe}_2\text{O}_3\text{-SiO}_2$ . *J Magn Magn Mater* 293: 533-536.
- 49 Rezlescu L, Rezlescu E, Popa PD, Rezlescu N (1999) Fine barium hexaferrite powder prepared by the crystallization of glass. *J Magn Magn Mater* 193: 288-290
- 50 Gornert P, Sinn E, Rosler M (1991) Crystalline materials: Growth and characterization 58: 129-148.
- 51 Abdel-Hameed SAM, Marzouk MA, Abdel-Ghany AE (2011) Magnetic properties of nanoparticles glass-ceramic rich with copper ions. *J Non-cryst solids* 357: 3888-3896
- 52 Safarikova M, Safarik I (2000) The application of magnetic techniques in biosciences. *Magn Electr Sep* 10: 223-252.
- 53 Babes L, Denizot B, Tanguy G, Jeune JLL, Jallet P (1999) Synthesis of iron oxide nanoparticles used as MRI contrast agents: a parametric study. *J Colloid Interface Sci* 212: 474-482.
- 54 Sun SH, Murray CB, Weller D, Folks L, Moser A (2000) Monodisperse FePt nanoparticles and ferromagnetic FePt nanocrystal superlattices. *Nature* 287: 1989-1992.
- 55 El-Shennawi AWA, Morsy AM, Serry MA (1990) Investigation of lithium magnesium-aluminosilicate solid solutions crystallized in some cordierite-zircon ceramics containing lithium. *J of Mat Sci* 25: 1429-1434.
- 56 Socoliuc V, Bica D, Vekas L (2003) Estimation of magnetic particle clustering in magnetic fluids from static magnetization experiments. *J. Colloid Interface Sci* 264: 141-147
- 57 Lu AH, Schmidt W, Matoussevitch N, Bönnemann H, Spliethoff B, et al. (2004) Nanoengineering of a magnetically separable hydrogenation catalyst. *Angew Chem Int Ed* 43: 4303-4306.
- 58 Sharifi I, Shokrollahi H, Amiri S (2012) Ferrite-based magnetic nanofluids used in hyperthermia applications. *J. Magn Magn Mater* 324: 903-915.
- 59 El-Shennawi AWA, Moris MM, Khater GA, Abdel-Hameed SAM (1998) Thermodynamic investigation of crystallization behavior of pyroxenic basalt-based glasses. *J Therm Anal* 51: 553-560.
- 60 Klug HP, Alexander LE (1974) X-Ray Diffraction procedures for polycrystalline and amorphous materials. Wiley New York.
- 61 Hammond C (1997) The Basic of crystallography and diffraction. Oxford university press, New York.
- 62 Scherrer P, Göttinger Nachrichten Gesell. (1918) 2: 98.
- 63 Patterson A (1939) The Scherrer Formula for X-Ray Particle Size Determination. *Phys Rev* 56: 978-982.
- 64 Myers HP (2002) Introductory Solid State Physics. Taylor & Francis.
- 65 Roy MK, Haldar B, Verma HC (2006) Characteristic length scales of nanosize zinc ferrite. *Nanotechnology* 17: 232.
- 66 Bretcanu O, Verne E, Coisson M, Tiberto P, Allia P (2006) Temperature effect on the magnetic properties of the coprecipitation derived ferromagnetic glass-ceramics. *Journal of Magnetism and Magnetic Materials* 300: 412-417.
- 67 Cullity RD (1972) Introduction of magnetic materials. Addison-Wesley.
- 68 Abdel-Hameed SAM, Rawhia LE (2012) Effect of  $\text{La}_2\text{O}_3$ ,  $\text{CoO}$ ,  $\text{Cr}_2\text{O}_3$  and  $\text{MoO}_3$  nucleating agents on crystallization behavior and magnetic properties of ferromagnetic glass-ceramic in the system  $\text{Fe}_2\text{O}_3\text{-CaO-ZnO-SiO}_2$ . *J Mater Res Bull* 47: 1233-1238.
- 69 Abdel-Hameed SAM, Ibrahim M Hamed, Nehal A. Erfan (2014) Utilization of iron oxide bearing pellets waste for preparing hard and soft ferromagnetic glass ceramics. *Journal of advanced ceramics* 3: 259-268